MOLECULAR AND CELLULAR BIOLOGY, Apr. 2008, p. 2244–2256 Vol. 28, No. 7
0270-7306/08/$08.00+0 doi:10.1128/MCB.01653-07

Functional Dissection of the NuA4 Histone Acetyltransferase Reveals Its Role as a Genetic Hub and that Eaf1 Is Essential for Complex Integrity▽

Leslie Mitchell,[1,2] Jean-Philippe Lambert,[1,2] Maria Gerdes,[1,2] Ashraf S. Al-Madhoun,[2] Ilona S. Skerjanc,[2] Daniel Figeys,[1,2] and Kristin Baetz[1,2]*

Ottawa Institute of Systems Biology, University of Ottawa, Ottawa, Ontario K1H 8M5, Canada,[1] and Department of Biochemistry, Microbiology and Immunology, University of Ottawa, Ottawa, Ontario K1H 8M5, Canada[2]

Received 6 September 2007/Returned for modification 22 October 2007/Accepted 8 January 2008

The *Saccharomyces cerevisiae* NuA4 histone acetyltransferase complex catalyzes the acetylation of histone H4 and the histone variant Htz1 to regulate key cellular events, including transcription, DNA repair, and faithful chromosome segregation. To further investigate the cellular processes impacted by NuA4, we exploited the nonessential subunits of the complex to build an extensive NuA4 genetic-interaction network map. The map reveals that NuA4 is a genetic hub whose function buffers a diverse range of cellular processes, many not previously linked to the complex, including Golgi complex-to-vacuole vesicle-mediated transport. Further, we probe the role that nonessential subunits play in NuA4 complex integrity. We find that most nonessential subunits have little impact on NuA4 complex integrity and display between 12 and 42 genetic interactions. In contrast, the deletion of *EAF1* causes the collapse of the NuA4 complex and displays 148 genetic interactions. Our study indicates that Eaf1 plays a crucial function in NuA4 complex integrity. Further, we determine that Eaf5 and Eaf7 form a subcomplex, which reflects their similar genetic interaction profiles and phenotypes. Our integrative study demonstrates that genetic interaction maps are valuable in dissecting complex structure and provides insight into why the human NuA4 complex, Tip60, has been associated with a diverse range of pathologies.

Histone acetyltransferase (HAT) enzyme complexes are key regulators of transcriptional control in all eukaryotic cells and have been linked to a diverse range of biological processes (reviewed in reference 61). HAT acetylation of specific lysines of N-terminal histone tails is believed to relieve DNA-protein interactions as well as to serve as a molecular beacon to attract additional chromatin remodeling or modifying proteins and/or transcription factors (reviewed in reference 34). In addition, the cellular processes regulated by HATs may not be governed solely by histone acetylation but, alternatively, may be mediated through the acetylation of nonhistone targets (reviewed in reference 23). To fully grasp the cellular implications of HATs will require both a comprehensive understanding of their diverse biological roles and a detailed understanding of the proteins within the complexes.

In *Saccharomyces cerevisiae*, the only essential HAT is the NuA4 complex. The known acetylation targets of NuA4 in vivo are histone H4 (1, 20, 58) and the histone H2A variant Htz1 (2, 28, 42). Similar to other HATs, NuA4 has been implicated in numerous nuclear events, including regulation of gene expression (reviewed in reference 18), DNA repair (reviewed in references 18 and 59), cell cycle progression (12, 13), and chromosome stability (31). Though the various cellular roles of NuA4 are likely mediated through H4 or Htz1 acetylation, the molecular mechanisms by which histone acetylation achieves diverse cellular functions is largely unknown. As the Tip60 complex, the human homolog of the yeast NuA4 complex, has numerous nonhistone targets (51), it is possible that some of the cellular functions of the yeast complex may be fulfilled through the acetylation of nonhistone substrates. Further, it is unlikely that all of the NuA4-mediated cellular functions have yet been defined. Indeed, NuA4 homologs in both humans and *Caenorhabditis elegans* have been implicated in a much broader range of cellular functions, including cytoplasmic roles in cell signaling (35, 51), suggesting that there may be roles for the yeast complex outside the nucleus.

NuA4 is composed of 13 subunits, including the essential acetyltransferase subunit Esa1 (13, 58; reviewed in reference 18). Of the other 12 NuA4 subunits, 5 are essential for cell viability (Act1, Arp4, Epl1, Swc4, and Tra1) and the remaining 7 are not (Eaf1, Eaf3, Eaf5, Eaf6, Eaf7, Yaf9, and Yng2) (reviewed in reference 18). Despite being the catalytic subunit, Esa1 on its own can target only free histones and is incapable of acetylating nucleosomes or chromatin (1, 7). As with other HAT enzyme complexes, the ability of Esa1 to target nucleosomes is dependent on complex formation. Esa1 has been isolated in two distinct complexes: the complete 13-subunit NuA4 complex and a trimer subcomplex composed of Esa1, Yng2, and Epl1 called Piccolo NuA4 (7). Studies suggest that Piccolo NuA4 cannot be recruited by transcription factors to specific locations, leading to the hypothesis that Piccolo NuA4 is responsible for nontargeted global histone acetylation, whereas the full NuA4 complex is responsible for targeted NuA4-dependent histone acetylation (7, 55).

* Corresponding author. Mailing address: Ottawa Institute of Systems Biology, Department of Biochemistry, Microbiology and Immunology, University of Ottawa, Roger Guidon Hall, 451 Smyth Rd., Ottawa, ONT K1H 8M5, Canada. Phone: (613) 562-5800, ext. 8592. Fax: (613) 562-5840. E-mail: kbaetz@uottawa.ca.

▽ Published ahead of print on 22 January 2008.

Esa1 and Yng2 interact independently with the N-terminal portion of Epl1, and it has been demonstrated that the N-terminal Enhancer of Polycomb A (EPcA) region of Epl1 and the N-terminal region of Yng2 are required for Esa1 to recognize and acetylate nucleosomes (7, 55). Though it is known that the C-terminal half of Epl1 is required to bridge Esa1 and Yng2 with the remaining 10 NuA4 subunits (7), very little is known regarding the physical interactions between the remaining NuA4 subunits. Studies have found that Yaf9 interacts with NuA4 through Swc4 in vivo (5), and both Eaf3 and Arp4 interact directly with Esa1 in vitro (21). As seen in other chromatin modification complexes, such as the SWR1 complex (67) and SWI/SNF (68), it is likely that the non-Piccolo NuA4 subunits may form multiple and distinct subcomplexes that perform a subset of the diverse NuA4 cellular functions.

The functional role of each individual NuA4 subunit remains to be fully understood, particularly with respect to the 10 non-Piccolo NuA4 subunits. One possibility is that some NuA4 subunits may be required for complex integrity, acting as a scaffold upon which other subunits bind. Alternatively, individual subunits or subcomplexes may be required for the targeted recruitment of NuA4 to distinct chromatin loci. Indeed, targeting roles have been characterized for some subunits. For example, upon DNA damage, Arp4 recognizes and interacts with histone H2A phosphorylated at serine 129. This action recruits NuA4 to regions of DNA double-strand breaks where histone H4 acetylation is required for DNA double-strand break repair (4, 17). Similarly, Tra1 directly interacts with the acidic transcriptional activators Gcn4, Hap4, and Gal4 (8). Further, Tra1 is required for both the acetylation of H4 surrounding the promoters and the transcription of Gcn4-dependent genes, suggesting that Tra1 may mediate the recruitment of NuA4 to certain promoters.

While specific targeting roles for the other subunits are undefined, the different phenotypes of the nonessential NuA4 subunits strongly support the hypothesis that different subunits are required for distinct NuA4 functions. For instance, while *yaf9*Δ, *yng2*Δ, and *eaf1*Δ cells display hypersensitivity to the microtubule-destabilizing drug benomyl, *eaf5*Δ and *eaf7*Δ cells display no sensitivity to this drug (30, 31, 36). Similarly, while *eaf1*Δ and *yaf9*Δ cells display high rates of chromosome loss (41 and 23 times greater than that of wild-type [WT] cells, respectively), *eaf3*Δ, *eaf5*Δ, *eaf6*Δ, and *eaf7*Δ cells display either no or only modest increases in their rates of chromosome loss compared to WT cells (31; L. Mitchell and K. Baetz, unpublished data).

Defining the roles of the individual subunits will provide critical insight into the NuA4 enzyme complex as a whole. In *S. cerevisiae*, a genetic method for exploring gene function is through the identification of synthetically lethal (SL) or synthetically sick (SS) genetic interactions by double mutant analysis. Mutants that are defective in the same essential or parallel nonessential pathways often display SL or SS interactions. The development of synthetic genetic array (SGA) analysis has enabled genetic screens to be performed systematically with yeast and has proven to be a powerful tool for predicting the cellular functions of a protein (63). Recently, subunits of NuA4 were analyzed in an epistatic miniarray profile (E-MAP) screen that identified pairwise genetic interaction between 743 genes implicated in various aspects of chromosome biology (14). This study solidified the role of NuA4 in its previously characterized functions, such as chromosome stability, DNA repair, transcription, and chromatin remodeling. However, given that the study was limited to genes involved in chromosome biology, no insights were gained into possible novel cellular functions of NuA4.

To comprehensively explore the global cellular functions of NuA4, we performed genome-wide SL-SGA analysis for five nonessential subunits. Our genetic interaction map reveals over 200 genetic interactions for the NuA4 subunits tested, dramatically expanding our knowledge of the potential cellular functions of the complex. Using the genetic interaction map, we identify a role for NuA4 in Golgi complex-to-vacuole vesicle-mediated transport. In addition, during our complex integrity studies, we discovered that NuA4 physically interacts with the stress response transcription factor Msn4. We also examine the effect of each nonessential subunit on NuA4 complex integrity and discover that the Eaf1 subunit, whose deletion is responsible for a large portion of the genetic interactions in our map, is essential for maintaining the complex integrity of NuA4. Moreover, Eaf5 and Eaf7, which display similar genetic interaction profiles and phenotypes, are found in a subcomplex. This integrative study provides novel insights into the pathways and processes impacted by NuA4 and sheds light on the roles of subunits within the complex.

MATERIALS AND METHODS

Yeast strains and plasmids. Yeast strains used in this study are listed in Table 1. The *MAT***a** deletion mutant array was purchased from Open Biosystems (catalog no. YSC1053). The SGA starting strain Y7092 (62) and the media used in the SL-SGA analysis have been described previously (63, 64). Genomic deletion or epitope tag integrations made for this study were designed with PCR-amplified cassettes as previously described (38, 47) and confirmed by PCR analysis. Plasmid pGST-*MSN4* (pKB1) was generated by PCR amplification of *MSN4* from genomic DNA using the primers 5′-ATCGGGATCCATGCTAGT CTTCGGACCTAATAG (forward) and 5′-GCATGCTCGAGTCAAAAATCA CCGTGCTTTTTG (reverse). The resulting PCR product was digested with BamHI and XhoI and ligated into pGEX6p-2 (Amersham Bioscience) also digested with BamHI and XhoI.

SL-SGA screens. Robotic manipulation of the deletion mutant array was conducted using a Singer RoToR HDA (Singer Instruments), and SL screens were performed as described previously (63). Genome-wide SL screens were conducted three times at 30°C for the following query strains: the *eaf1*Δ, *eaf3*Δ, *eaf5*Δ, *eaf6*Δ, and *eaf7*Δ strains. The resultant double mutants were scored for SL or SS interactions by visual inspection. For the *eaf1*Δ screen, putative genetic interactions, identified in a minimum of two out of three screens, were confirmed by tetrad dissection on yeast-peptone-dextrose (YPD) medium at 25°C. For the *eaf3*Δ, *eaf5*Δ, *eaf6*Δ, and *eaf7*Δ screens, only those putative interactions identified in a minimum of two out of three screens that had not been previously published (as listed at www.thebiogrid.org as of April 2007) were confirmed by tetrad dissection, as described above. Any published interactions in the BioGrid database that were not identified in our screens were incorporated into our data set. The complete list of interactions and references are provided at www.oisb.ca/personal_web_site/Baetz_Lab/publicationsFS.html.

NuA4 PrA-tagged protein purification and identification. One-step affinity purification of protein A (PrA; one epitope of the tandem affinity purification [TAP] tag)-tagged NuA4 components was performed. Cells from 200 ml of mid-log-phase culture (optical density at 600 nm [OD_{600}], ~0.6 to 0.8) grown in YPD at 25°C were collected by centrifugation, washed in 10 ml lysis buffer (20 mM HEPES, pH 7.4, 0.1% Tween 20, 2 mM $MgCl_2$, 300 mM NaCl, protease inhibitor cocktail [P-8215; Sigma]) and transferred to a 1.5-ml Eppendorf tube. Cells were resuspended in 300 μl lysis buffer plus an equal volume of acid-washed glass beads (catalog no. 35-535; Fisher Scientific), and cells were lysed through vortexing (six 1-min blasts with incubation on ice in between vortexing). The soluble whole-cell extract (WCE) was isolated by centrifugation at 13,200 rpm for 20 min. Ten milligrams of the WCE was incubated with 25 μl of magnetic

TABLE 1. Yeast strains used in this study

Strain	Auxotrophies	Reference or source
YPH499	*MAT***a** *ura3-52 lys2-801 ade2-101 trp1-Δ63 his3-Δ200 leu2-Δ1*	57
Y7092	*MATα can1Δ::STE2pr-*Sp_*his5 lyp1Δ his3Δ1 leu2Δ0 ura3Δ0 met15Δ0*	64
YKB622	*MATα can1Δ::STE2pr-*Sp_*his5 lyp1Δ his3Δ1 leu2Δ0 ura3Δ0 met15Δ0 eaf1Δ::NAT*	31
YKB995	*MATα can1Δ::STE2pr-*Sp_*his5 lyp1Δ his3Δ1 leu2Δ0 ura3Δ0 met15Δ0 eaf3Δ::NAT*	This study
YKB852	*MATα can1Δ::STE2pr-*Sp_*his5 lyp1Δ his3Δ1 leu2Δ0 ura3Δ0 met15Δ0 eaf5Δ::NAT*	31
YKB623	*MATα can1Δ::STE2pr-*Sp_*his5 lyp1Δ his3Δ1 leu2Δ0 ura3Δ0 met15Δ0 eaf6Δ::NAT*	Gift from J. Greenblatt
YKB853	*MATα can1Δ::STE2pr-*Sp_*his5 lyp1Δ his3Δ1 leu2Δ0 ura3Δ0 met15Δ0 eaf7Δ::NAT*	31
LPY3500	*MAT***a** *his3Δ200 leu2-3,112 trp1Δ1 ura3-52 esa1Δ::HIS3 esa1(L245P)::URA3*	13
KLY35	*MATα can1Δ::STE2pr-*Sp_*his5 lyp1Δ his3Δ1 leu2Δ0 ura3Δ0 met15Δ0 LYS2$^+$ htz1-ND-loxP::NAT*	Gift from M. C. Keogh
YKB625	*MATα can1Δ::STE2pr-*Sp_*his5 lyp1Δ his3Δ1 leu2Δ0 ura3Δ0 met15Δ0 htz1Δ::NAT*	This study
YKB1007	*MAT***a** *ura3-52 lys2-801 ade2-101 trp1-Δ63 his3-Δ200 leu2-Δ1 EAF1-TAP::TRP*	This study
YKB44	*MAT***a** *ura3-52 lys2-801 ade2-101 trp1-Δ63 his3-Δ200 leu2-Δ1 eaf1Δ::kanMX*	This study
YKB654	*MAT***a** *ura3-52 lys2-801 ade2-101 trp1-Δ63 his3-Δ200 leu2-Δ1 eaf3Δ::TRP*	This study
YKB658	*MAT***a** *ura3-52 lys2-801 ade2-101 trp1-Δ63 his3-Δ200 leu2-Δ1 eaf5Δ::TRP*	This study
YKB662	*MAT***a** *ura3-52 lys2-801 ade2-101 trp1-Δ63 his3-Δ200 leu2-Δ1 eaf6Δ::TRP*	This study
YKB464	*MAT***a** *ura3-52 lys2-801 ade2-101 trp1-Δ63 his3-Δ200 leu2-Δ1 yaf9Δ::kanMX*	This study
YKB494	*MAT***a** *ura3-52 lys2-801 ade2-101 trp1-Δ63 his3-Δ200 leu2-Δ1 yng2Δ::kanMX*	This study
YKB500	*MAT***a** *ura3-52 lys2-801 ade2-101 trp1-Δ63 his3-Δ200 leu2-Δ1 htz1Δ::kanMX*	This study
YKB1035	*MAT***a** *ura3-52 lys2-801 ade2-101 trp1-Δ63 his3-Δ200 leu2-Δ1 MSN4-TAP::TRP*	This study
YKB518	*MAT***a** *ura3-52 lys2-801 ade2-101 trp1-Δ63 his3-Δ200 leu2-Δ1EAF7-MYC::kanMX*	This study
YKB1069	*MAT***a** *ura3-52 lys2-801 ade2-101 trp1-Δ63 his3-Δ200 leu2-Δ1 msn4-TAP::TRP EAF7-MYC::kanMX*	This study
YKB440	*MAT***a** *Δtrp ura3-1 leu2-3,112 his3-11,15 ade2-1 can1-100 ESA1-TAP::TRP*	Gift from N. Krogan
YKB1091	*MAT***a** *ura3-52 lys2-801 ade2-101 trp1-Δ63 his3-Δ200 leu2-Δ1 msn4-TAP::TRP eaf1Δ::kanMX*	This study
YKB855	*MAT***a** *ESA1-TAP::TRP eaf1Δ::kanMX*	This study
YKB765	*MAT***a** *Δtrp ura3-1 leu2-3,112 his3-11,15 ade2-1 can1-100 ESA1-TAP::TRP eaf3Δ::kanMX*	This study
YKB854	*MAT***a** *Δtrp ura3-1 leu2-3,112 his3-11,15 ade2-1 can1-100 ESA1-TAP::TRP eaf5Δ::kanMX*	This study
YKB766	*MAT***a** *Δtrp ura3-1 leu2-3,112 his3-11,15 ade2-1 can1-100 ESA1-TAP::TRP eaf6Δ::kanMX*	This study
YKB964	*MAT***a** *Δtrp ura3-1 leu2-3,112 his3-11,15 ade2-1 can1-100 ESA1-TAP::TRP eaf7Δ::kanMX*	This study
YKB966	*MATα ESA1-TAP::TRP yaf9Δ::kanMX*	This study
YKB967	*MATα ESA1-TAP::TRP yng2Δ::kanMX*	This study
YKB1054	*MAT***a** *esa1-TAP::TRP EAF7-MYC::kanMX*	This study
YKB1043	*MAT***a** *esa1-TAP::TRP EAF7-MYC::kanMX eaf5Δ::kanMX*	This study
YKB442	*MAT***a** *his3Δ1 leu2Δ0 met15Δ0 ura3Δ0 EAF7-TAP::HIS*	TAP collection
YKB1034	*MAT***a** *EAF7-TAP::HIS eaf1Δ::kanMX*	This study
YKB1097	*MAT***a** *ura3-52 lys2-801 ade2-101 trp1-Δ63 his3-Δ200 leu2-Δ1 msn2Δ::TRP msn4Δ::kanMX eaf1Δ::kanMX*	This study

Dynabeads (catalog no. 143-01; Dynal, Invitrogen) crossed-linked to rabbit immunoglobulin G (IgG) (catalog no. PP64; Chemicon) as per Invitrogen's instructions. Following 2 hours of end-over-end incubation at 4°C, Dynabeads were collected with a magnet and washed five times with 1 ml cold lysis buffer. The Dynabeads were resuspended in 25 μl of modified 1× loading buffer (50 mM Tris, pH 6.8, 2% sodium dodecyl sulfate [SDS], 0.1% bromophenol blue, 10% glycerol), and PrA-tagged proteins and copurifying proteins were eluted from the beads with moderate heat (65°C for 10 min). Loading buffer was transferred to a new tube, and 2-β-mercaptoethanol was added to a final concentration of 200 mM. Samples were boiled for 5 min, and 20 μl was resolved on 4 to 12% polyacrylamide gradient gels (catalog no. NP0321BOX; Invitrogen) in 1× MES (morpholineethanesulfonic acid) buffer. Proteins were visualized by silver staining.

Immunoprecipitation and immunoblotting. PrA purification of Msn4-TAP was performed as described above except 15 mg of WCE was incubated with the IgG-coated Dynabeads overnight. Immunoprecipitations were separated by 7.5% SDS-polyacrylamide gel electrophoresis (PAGE). Standard Western blotting procedures were performed using the following antibodies: anti-TAP (CAB1001; Open Biosystems), anti-Myc (catalog no. 11667149; Roche), peroxidase-conjugated goat anti-rabbit IgG (catalog no. AP307P; Chemicon), and peroxidase-conjugated goat anti-mouse IgG (catalog no. 170-6516; Bio-Rad). In cases where the anti-TAP antibody cross-reacted with the IgG eluted from the magnetic beads, the anti-TAP antibody was conjugated to horseradish peroxidase using the SureLINK horseradish peroxidase conjugation kit (catalog no. 84-00-01; KPL) as per the manufacturer's instructions.

Mass spectrometric detection of proteins by liquid chromatography-MS/MS. Gel bands were excised and subjected to in-gel tryptic digestion by following standard protocols (56). For the knockout analysis, in cases where bands were missing, areas corresponding to the missing bands were also excised to confirm that the proteins were truly missing. Liquid chromatography-tandem mass spectrometry (MS/MS) was performed using the LTQ quadrupole ion trap mass spectrometer (Thermo-Electron, Waltham, MA) as described previously (50). MS/MS data were analyzed and matched to *S. cerevisiae* protein sequences in the NCBI nonredundant database using the Mascot database search engine (Matrix Science Inc., Boston, MA).

Fluorescence microscopy. Cells grown at 25°C in YPD medium were resuspended at 2 to 4 OD_{600} U/ml and stained with FM4-64 (catalog no. T35356; Molecular Probes) at a final concentration of 20 μM for 25 min at 30°C. Cells were resuspended in fresh medium and incubated at 30°C for a 2-h chase period. The *esa1*(*L254P*) cells were incubated at 37°C for the chase period. Cells were then resuspended at 4 to 8 OD_{600} U/ml in fresh YPD medium. Slides were analyzed with a Leica DM IRE2 microscope using a 625-nm filter. Images were acquired using a Retiga 12-bit camera (Leica) and analyzed using Improvision 3.1 software.

In vitro binding assay. Msn4 fused to glutathione *S*-transferase (GST) (pKB1) as well as GST alone (pGEX-6P2; Amersham) was purified from *Escherichia coli* on glutathione-Sepharose as recommended by Amersham. GST-Msn4 and GST protein concentrations were normalized by Coomassie blue staining on 10% SDS-PAGE gels. The NuA4 complex from yeast cells expressing Esa1-TAP or background control (WT) yeast cells with no TAP-tagged proteins was purified using IgG-coated magnetic Dynabeads as described above. Twenty-five microliters of Dynabeads complexed with NuA4 (Esa1-TAP), the background (WT) protein, or beads alone was equilibrated twice with 1-ml washes in cold binding buffer (20 mM HEPES, pH 7.4, 0.001% Tween 20, 2 mM $MgCl_2$, 100 mM NaCl). Equivalent amounts of GST and GST-Msn4 were then incubated with NuA4, the WT protein, or Dynabeads alone for 2 h at 4°C with end-over-end rotation in a

volume of 500 μl. Dynabeads were washed twice with 1 ml cold binding buffer and then five times with 1 ml cold lysis buffer (see above). Proteins were eluted as described above and resolved by 10% SDS-PAGE. Anti-GST Western blots were carried out with anti-GST (catalog no. A5800; Invitrogen) and peroxidase-conjugated goat anti-rabbit IgG (catalog no. AP307P; Chemicon) using standard procedures.

Modified ChIP. TAP-tagged and untagged strains, grown in YPD medium at 25°C to an OD_{600} of 0.8, were collected by centrifugation, washed with 5 ml chromatin immunoprecipitation (ChIP) lysis buffer (100 mM HEPES, pH 8.0, 20 mM magnesium acetate, 10% glycerol, 0.1 mM EDTA, protease inhibitor cocktail [catalog no. P-8215; Sigma]) and transferred to 1.5-ml Eppendorf tubes. Cells were resuspended in 500 μl lysis buffer plus an equal volume of acid-washed glass beads (catalog no. 35–535; Fisher Scientific) and lysed by vortexing (six 1-min blasts, with incubation on ice in between vortexing). The crude WCE was separated from the beads into a fresh Eppendorf tube by centrifugation at 1,000 rpm for 1 min through a hole in the bottom of the Eppendorf tube created using a red-hot 18-gauge needle. Samples were subjected to three rounds of sonication (10 seconds each) (Sonic Dismembrator model 60, at setting 2; Fisher Scientific), with a 30-second incubation on ice between each pulse. NP-40 was added to each sample to a final concentration of 1%. Samples were clarified by centrifugation at 3,000 rpm for 10 min at 4°C. One hundred micrograms of WCE was reserved to serve as an "input" control, while 10 mg of WCE was incubated overnight at 4°C with 25 μl of IgG-coated Dynabeads as described above. Beads were washed three times with 1 ml cold ChIP wash buffer (ChIP lysis buffer plus 0.5% NP-40). Twenty percent of the beads were reserved to test for immunopurification of the TAP-tagged proteins by Western blotting as described above. The remainder of the beads and the input WCE were treated with protease K (0.5 mg/ml in Tris-EDTA) for 2 h at 37°C. Protein was extracted using phenol-chloroform, and DNA was ethanol precipitated in the presence of 1 μg of glycogen. DNA pellets were washed with 70% ethanol, air dried, and resuspended in 50 μl of Tris-EDTA. Immunoprecipitated DNA was amplified using multiplex PCR with the following primer pairs: *HSP12* F (5′ CGCAAGCATTAATACAACCC) and *HSP12* R (5′ CGCAATTGAGGAAGTAGAAC) and Chr V no-ORF F (5′ GGCTGTCAGAATATGGGGCCGTAGTA) and Chr V no-ORF R (5′ CCCC GAAGCTGCTTTCACAATAC). PCR products were resolved on a 2% agarose gel and visualized with ethidium bromide.

Northern blot analysis. Yeast strains were grown at 25°C in YPD medium to an OD_{600} of 0.6 to 0.9. Heat shock conditions were carried out at 39°C for 30 min. RNA was isolated using a hot-phenol extraction method (53), except that TES acid buffer (10 mM Tris-HCl, pH 7.5, 10 mM EDTA, pH 8.0, 0.5% SDS) was used, and samples were incubated at 65°C for 1 h. Northern blotting was carried out as previously described (3). The probes used for the Northern blot analysis were created by PCR amplification of the coding sequences of *HSP12* (5′ GTCTGACGCAGGTAGAAAAGG [forward], 5′ CGCAAGCATTAATACA ACCC [reverse]) and *ACT1* (5′ GCATCATACCTTCTACAACG [forward], 5′ GTGATGACTTGACCATCTGG [reverse]). Probes were labeled using the Megaprime DNA labeling system (catalog no. RPN1607; Amersham) in the presence of [α-^{32}P]dCTP (GE Healthcare).

RESULTS

An extensive NuA4 genetic-interaction map indicates that NuA4 impacts a diverse range of cellular processes. In an effort to comprehensively identify the cellular processes potentially impacted by NuA4, we performed genome-wide SL screens using query strains with deletions of all seven nonessential NuA4 genes (*eaf1*Δ, *eaf3*Δ, *eaf5*Δ, *eaf6*Δ, *eaf7*Δ, *yaf9*Δ, and *yng2*Δ). All seven genome-wide SL screens were performed in triplicate using SGA methodology by mating each query strain to the yeast deletion mutant array and selecting for double mutants (63). Any double mutant combinations that resulted in inviability (SL) or in reduced fitness (SS) that were identified in a minimum of two out of three screens were confirmed by tetrad analysis (genetic interaction data set available at www.oisb.ca/personal_web_site/Baetz_Lab/publicationsFS.html). Despite multiple attempts with *yng2*Δ and *yaf9*Δ query strains, reproducible genetic-interaction profiles were not obtained. The resulting confirmed data set contains 172 genetic interactions among 149 genes, of which 18% (31/172) were SL interactions and the remainder were SS interactions. To increase the coverage of our data set, we also incorporated *eaf1*Δ, *eaf3*Δ, *eaf5*Δ, *eaf6*Δ, or *eaf7*Δ genetic interactions confirmed in previously published SL-SGA analyses or direct testing (see Materials and Methods for details). The combined data set contains 268 genetic interactions among 204 genes, of which 38% (101/268) were SL interactions and the remainder were SS interactions.

Given that genetic interactions predict functional relationships (63), the NuA4 genetic interaction map identified many genes that encode proteins implicated in cellular processes previously associated with the NuA4 complex, including chromatin structure, transcription, DNA repair, and chromosome stability, as determined by their gene ontology (GO) annotations (Fig. 1). Significantly, the NuA4 genetic map enriched for genes encoding proteins within the same protein complexes, suggesting that our screening method provided extensive coverage of the genome and thus the ability to predict interactions between NuA4 and protein complexes. Some examples of this are the SAGA complex (*GCN5*, *SGF9*, *SGF73*, *SGF11*), the SWR complex (*ARP6*, *SWC3*, *SWC5*, *SWR1*, *VPS71*, *VPS72*), and the MRX complex (*MRE11*, *RAD50*, *XRS2*). This is the first time that genetic interactions have been identified for any NuA4 subunit on a genome-wide scale, so in addition to supporting the well-characterized roles for NuA4, the genetic interaction map enriched for numerous other genes implicated in a wide variety of functions, including vesicle-mediated transport, stress response, and arginine biosynthesis.

Eaf1 functions primarily as a component of NuA4. Although it has been shown that genes that function within the same protein complex have similar genetic interaction profiles (14), we observed that the five NuA4 subunits have remarkably different genetic interaction profiles, particularly with respect to the total number of genetic interaction partners. While *eaf3*Δ, *eaf5*Δ, *eaf6*Δ, and *eaf7*Δ mutants genetically interacted with 31, 42, 12, and 35 genes, respectively, the *eaf1*Δ mutant genetically interacted with 148 genes. Further, 75% of the *eaf1*Δ genetic interactions were specific to the *eaf1*Δ mutant alone (genetic interaction data set available at www.oisb.ca/personal_web_site/Baetz_Lab/publicationsFS.html). This suggests that either Eaf1 plays a crucial role in NuA4 that is not shared by the other nonessential subunits tested or Eaf1 functions on its own or as part of an additional protein complex(es). Previous studies were not able to identify copurifying proteins when tagged Eaf1 was used as bait (22, 32). Therefore, to test the hypothesis that Eaf1 is found only in NuA4, we immunopurified a TAP-tagged version of Eaf1 and identified its interacting proteins using a modified procedure (Fig. 2). One-step purification was performed using IgG-coated magnetic beads that interact with the PrA component of the TAP tag. Proteins were eluted from the beads in sample buffer at 65°C, separated by SDS-PAGE, and silver stained. This protocol results in low-level background binding of nonspecific proteins to IgG beads (Fig. 2, WT lane) and a high yield of TAP purifications. Protein bands were individually cut, and MS was performed to identify the Eaf1-TAP-interacting proteins. We discovered that Eaf1-TAP copurifies only with subunits of the NuA4 complex and Fks1, which was identified in all NuA4 purifications using this protocol (Fig. 2 and see Fig. 5 and 6).

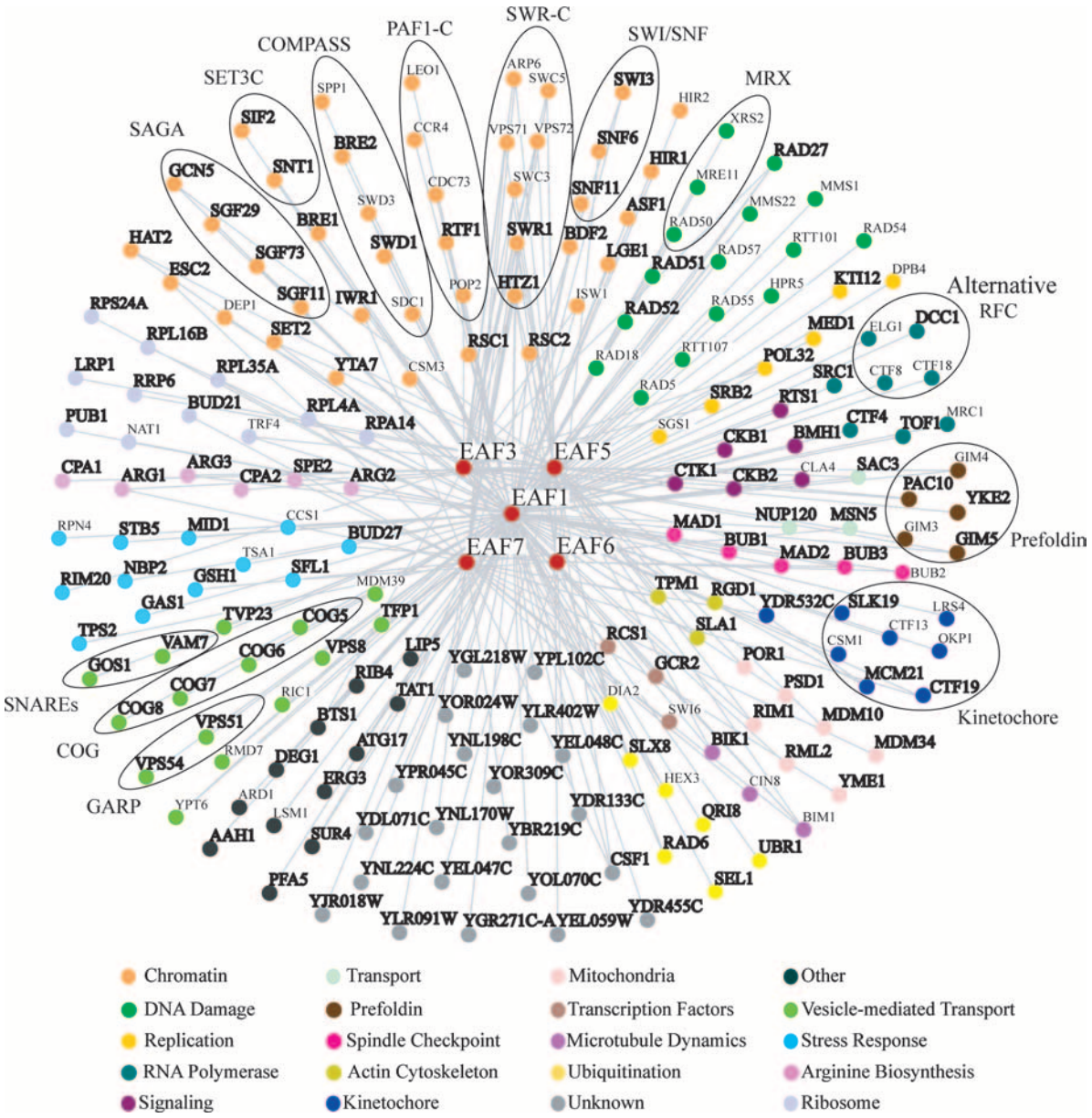

FIG. 1. Synthetic genetic-interaction map of five NuA4 subunits. Genome-wide SL-SGA screens were performed using query strains for five nonessential NuA4 subunits: the *eaf1*Δ (YKB622), *eaf3*Δ (YKB993), *eaf5*Δ (YKB852), *eaf6*Δ (YKB623), and *eaf7*Δ (YKB853) strains. The 199 NuA4-interacting genes are represented by nodes that are color coded based on the GO process. Gray lines indicate genetic interactions (both SS and SL interactions). The 139 interacting genes highlighted in bold text indicate those genes whose interaction with at least one NuA4 query strain was confirmed by tetrad dissection in our lab. The remaining interacting genes in the map represent previously published genetic interactions that were either identified in our SGA screens but were not confirmed by tetrad dissection or not identified in our screens. Genes encoding subunits of a single protein complex are grouped together with black circles.

As Fks1, a subunit of the 1,3-beta-D-glucan synthase enzymatic complex (29), localizes to the plasma membrane and has not previously been reported to interact with NuA4, we suspect that this interaction is an artifact of the purification procedure.

Since Eaf1-TAP copurified only with NuA4 proteins (and Fks1), this suggests that the 148 *eaf1*Δ genetic interactions are attributable to Eaf1's role in NuA4. Hence, we hypothesized that the *eaf1*Δ genetic interactions would be largely shared with a strain with a mutation in the essential NuA4 catalytic subunit Esa1. To test this, we directly mated the *esa1*(*L245P*) mutant (13), a temperature-sensitive point mutant that displays acetylation defects, with 148 deletion mutants that displayed genetic interactions with the *eaf1*Δ strain. Diploids were sporulated, and tetrads were dissected at 25°C. Of the 148 matings, 140 produced reliable tetrads. Dot assays were performed at 30°C to test for synthetic genetic interactions of these double mutants, except for three double mutants that proved to be SL or extremely SS on the dissection plates (the *YKE2*, *TPM1*, and *RIB4* mutants). Nineteen displayed no growth phenotype defects in combination with the *esa1*(*L245P*) mutation at 30°C,

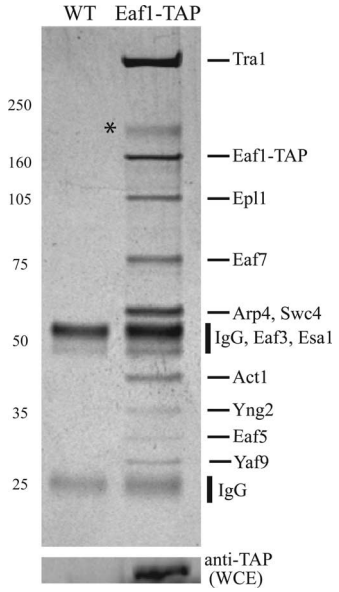

FIG. 2. Eaf1-TAP purifies the NuA4 complex. SDS-PAGE (gradient gel) and silver staining comparing NuA4 that was affinity purified via Eaf1-TAP (YKB1007) and NuA4 from an untagged strain (WT; YPH499), using IgG-coated magnetic beads that bind the PrA component of the TAP tag. IgG heavy and light chains coelute upon heating. Protein bands were identified by MS as indicated. Eaf6 was not efficiently silver stained. The * indicates a non-NuA4, copurifying protein, Fks1. Anti-TAP Western blotting demonstrates the expression of Eaf1-TAP in the WCE. This gel is representative of those from three purification experiments. Numbers at the left indicate molecular masses (in kDa).

while the remaining 118 deletion mutants were either SL or SS in combination with the *esa1*(*L245P*) mutation (see Suplemental Table2 at www.oisb.ca/personal_web_site/Baetz_Lab/publicationsFS.html). The facts that 86% of *eaf1*Δ genetic interactions are shared with the acetylation-deficient *esa1*(*L245P*) mutant and that Eaf1-TAP copurifies only with NuA4 suggest that Eaf1 functions primarily as a component of NuA4.

NuA4 function impacts vesicle-mediated transport. Surprisingly, the NuA4 genetic map identified 15 genes that encode proteins with well-established roles in vesicle-mediated transport (Fig. 1 and Table 2). Remarkably, most of the vesicle-mediated transport gene deletions displayed only genetic interactions with *eaf1*Δ and the *esa1*(*L245P*) catalytically deficient mutant (Table 2). Indeed, no genetic interactions were identified between *eaf3*Δ or *eaf6*Δ mutants and this group of genes. Further, of the 13 *eaf1*Δ mutant genetic interactions with the vesicle-mediated transport genes, eight were SL, including the interactions with all four nonessential subunits of the conserved oligomeric Golgi complex (*COG5*, *COG6*, *COG7*, *COG8*) (reviewed in reference 65), the soluble *N*-ethylmaleimide-sensitive factor attachment protein receptors (*GOS1* and *VAM7*) (reviewed in reference 26), the Golgi complex-associated retrograde protein complex subunit (*VPS54*) (reviewed in reference 44), and the GTPase (*YPT6*) (reviewed in reference 46). Many of the vesicle-mediated transport genes identified have specific roles in Golgi complex-to-vacuole transport, and deletion of most of these genes results in altered vacuole morphology (54). The strong genetic interactions of *eaf1*Δ and *esa1*(*L245P*) with these mutants suggest that NuA4 may impact vesicle-mediated transport and that NuA4 mutants may also display aberrant vacuole morphology. To test this hypothesis, we examined vacuolar morphology in all seven nonessential NuA4 mutants and the *esa1*(*L245P*) mutant using the fluorescent vacuolar vital stain FM4-64 (66). As expected *eaf3*Δ, *eaf5*Δ, *eaf6*Δ, and *eaf7*Δ cells, which do not have any or have only a few genetic interactions with vesicle-mediated transport genes, displayed vacuole morphology similar to that of the WT (Fig. 3A). In contrast, *eaf1*Δ, *yaf9*Δ, *yng2*Δ, and *esa1*(*L245P*) cells displayed altered vacuole morphology, with the majority of cells displaying one large vacuole (Fig. 3A). This suggests that Eaf1, Yaf9, Yng2, and the acetyltransferase activity of Esa1 are required for vacuole function. As NuA4 may mediate some of its cellular roles through Htz1 acetylation (2, 28, 42) and *htz1*Δ mutants display some phenotypes similar to those of NuA4 mutants (30, 31), we next tested whether *htz1*Δ and *htz1-ND* cells, in which the N-terminal amino acids 3 to 14 (KAHGGKGKSGAK) are replaced with 24 amino acids (CRSTTLNITSYNVCYTKLLGDIRT), also display defects in vacuole morphology. While the majority of *htz1*Δ cells displayed large vacuoles similar to those of *eaf1*Δ, *yaf9*Δ, *yng2*Δ, and *esa1*(*L245P*) cells, the *htz1-ND* cells displayed WT vacuole morphology (Fig. 3B). This suggests that the Htz1 globular core, but not the N terminus or N-terminal acetylation sites, is required for vacuole function. We next directly tested whether *htz1*Δ mutants display synthetic genetic interactions with a subset of the identified deletion mutants which interact with both *eaf1*Δ and *esa1*(*L245P*) mutant: the *TVP23*, *VPS51*, *GOS1*, *VPS8*, and *COG6* mutants. *htz1*Δ mutants shared all these genetic interactions (Fig. 3C). This suggests that both NuA4 and Htz1 have a role in vesicle-mediated transport, likely through the transcriptional regulation of a key gene(s) required for vesicle-mediated transport.

TABLE 2. Genetic interactions of NuA4 mutants with vesicle-mediated transport genes

Interacting gene	Phenotype with indicated NuA4 gene[a]			
	EAF1	*ESA1*	*EAF5*	*EAF7*
GOS1	SL	SL		
VAM7	SL	SS		
TVP23	SS	ND		
TFP1		ND		SS
VPS8	SS	SS		
COG5	SL	SS		
COG6	SL	SL		
COG7	SL	SL		
COG8	SL	SL		
RIC1		ND		SL
RMD7	SS	ND		
YPT6	SL	SS		SL
VPS51	SS	SS	SS	
VPS54	SL	SL		
MDM39	SS	ND		

[a] Empty spaces indicate that no genetic interaction was found by genome-wide SL-SGA screens. ND indicates that no data were obtained from *esa1*(*L245P*) mutant direct tests either because the gene was not identified in the *eaf1*Δ cell screen (*TFP1* and *RIC1*) or reliable tetrads were not obtained (*TVP23*, *RMD7*, and *MDM39*). *eaf3*Δ and *eaf6*Δ mutants did not display genetic interactions with any of the vesicle-mediated transport genes.

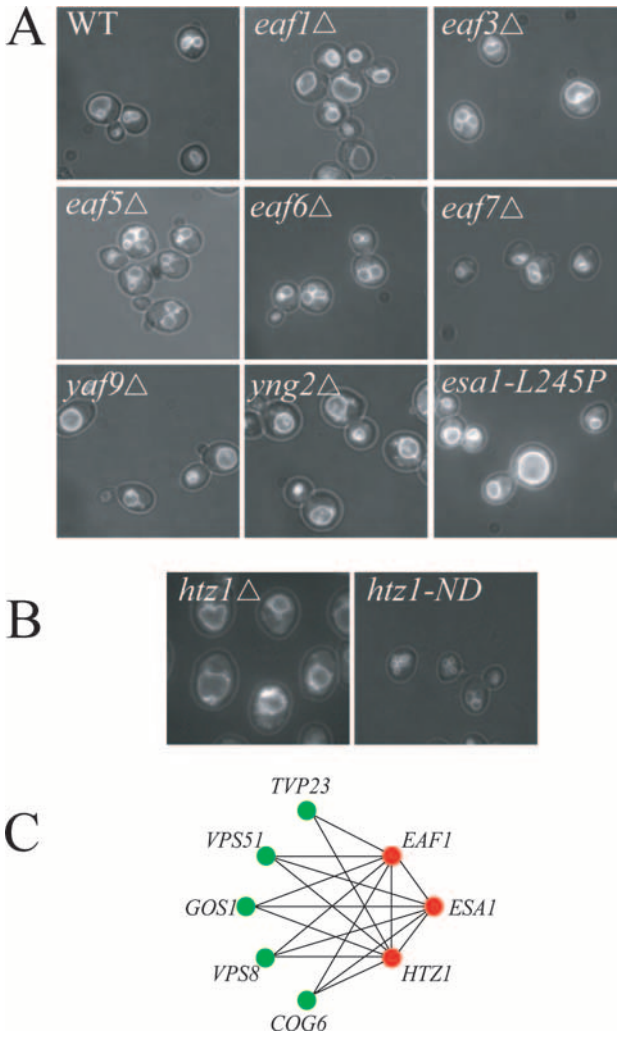

FIG. 3. NuA4 function impacts vesicle-mediated transport. (A) *eaf1*Δ, *yaf9*Δ, *yng2*Δ, and *esa1*(*L245P*) cells display vacuolar-morphology defects. Vacuole morphology was examined in WT (YPH499) cells, in strains deficient in each of the seven nonessential NuA4 subunits (*eaf1*Δ [YKB44], *eaf3*Δ [YKB654], *eaf5*Δ [YKB658], *eaf6*Δ [YKB662], *eaf7*Δ [YKB853], *yaf9*Δ [YKB464], and *yng2*Δ [YKB494]), and in a temperature-sensitive point mutant of the catalytic subunit [*esa1*(*L245P*) (LPY3500)] using the dye FM4-64. The WT and deletion mutants were grown at 30°C, while *esa1*(*L245P*) mutants were grown at 37°C for 2 h after FM4-64 treatment. Images shown were taken after the merger of fluorescent light and transmitted light. (B) *htz1-ND* cells (YKL35) do not show vacuolar-morphology defects, while *htz1*Δ (YKB625) cells display defects similar to those of the *eaf1*Δ, *yaf9*Δ, *yng2*Δ, and *esa1*(*L245P*) mutants. Vacuole morphology was examined in mutant cells with FM4-64 as described for panel A. (C) *htz1*Δ (YKB500), *esa1*(*L245P*) (LPY3500), and *eaf1*Δ (YKB622) mutants (indicated by the red dots) genetically interact with a subset of vesicle-mediated transport genes (indicated by green dots) identified in the NuA4 SGA screens. Lines connect genes with synthetic genetic interactions.

NuA4 and the stress-responsive transcription factor Msn4. The genetic interaction map also identified 10 genes that have been implicated in the yeast stress response, thereby suggesting a functional connection between NuA4 and the stress response (Fig. 1). Additionally, during the course of our analysis of NuA4 complex integrity (see below), we identified the general stress-responsive transcription factor Msn4, which comigrates with Esa1-TAP, in four separate Esa1-TAP purifications. Msn4, along with its functionally related homolog Msn2, are required for the transcriptional induction of numerous stress response genes upon various environmental and metabolic cues (39). We were also interested in the physical interaction between NuA4 and Msn4 because microarray analysis of several NuA4, SWR, and Isw1 mutants previously demonstrated that the complex plays a role in the transcriptional repression of a large number of Msn2/4-dependent stress response genes (25, 37). Further, it was demonstrated that the derepression of a subset of Msn2/4 target genes in NuA4, SWR, or Isw1 mutants in the absence of environmental stress requires Msn2 and/or Msn4 (37). Having initially identified the physical interaction between NuA4 and Msn4 by MS, we sought to test the validity of the interaction in vivo by reciprocal immunopurification of NuA4 using a tagged version of Msn4. To accomplish this, we generated a strain expressing both Msn4-TAP and Eaf7-Myc from their endogenous promoters. IgG-coated magnetic beads were used to immunopurify Msn4-TAP, and Western blot analysis confirmed the presence of Eaf7-Myc (Fig. 4A). Given that Eaf7 has been identified only within the NuA4 complex, we conclude that Msn4 physically interacts directly or indirectly with the NuA4 enzyme complex. Though Msn4 and Msn2 migrate at the same rate on SDS-PAGE gels, we never identified Msn2 by MS in our Esa1-TAP purification. However, as Msn2 and Msn4 are largely redundant, we also asked whether NuA4 and Msn2 interact. Experiments using Msn2-TAP showed that Msn2-TAP coimmunoprecipitates Eaf7-Myc (data not shown), indicating the NuA4 interacts with both Msn2 and Msn4. While this experiment verified the interaction between NuA4 and both Msn4 and Msn2, it told us little about whether the interaction is mediated by other, non-NuA4 proteins. As Msn2 and Msn4 likely act in the same manner, the remaining experiments were performed with Msn4 alone. To test whether the physical interaction between NuA4 and Msn4 is direct, we performed an in vitro binding experiment using recombinant GST-Msn4 purified from *E. coli* and NuA4 isolated from yeast using IgG-coated magnetic beads after extensive washes. We found that while GST alone does not bind to NuA4, GST-Msn4 specifically interacts with the NuA4 enzyme complex (Fig. 4B), suggesting that the interaction between Msn4 and the NuA4 enzyme complex is likely direct. However, although we believe our NuA4 immunopurification to be extremely clean (Fig. 5A), given that NuA4 was purified from yeast, we cannot rule out the possibility that non-NuA4 copurifying proteins mediated the interaction with Msn4.

In light of the physical interaction between NuA4 and Msn4/Msn2 and the derepression of a subset of Msn2/4 genes in NuA4 mutants, we next decided to further explore the molecular mechanism connecting Msn2/4 and NuA4. Under non-stress conditions, the majority of Msn2 and Msn4 proteins are localized to the cytoplasm, and upon environmental stress, they enter the nucleus and bind to stress response elements upstream of their target genes (24). However, strains with mutations in NuA4 do not display increased Msn2 or Msn4 nuclear localization, nor is the H4 acetylation of the promoters of derepressed Msn4/2 target genes significantly changed from that of control promoters in *yaf9*Δ cells (37). This suggests that

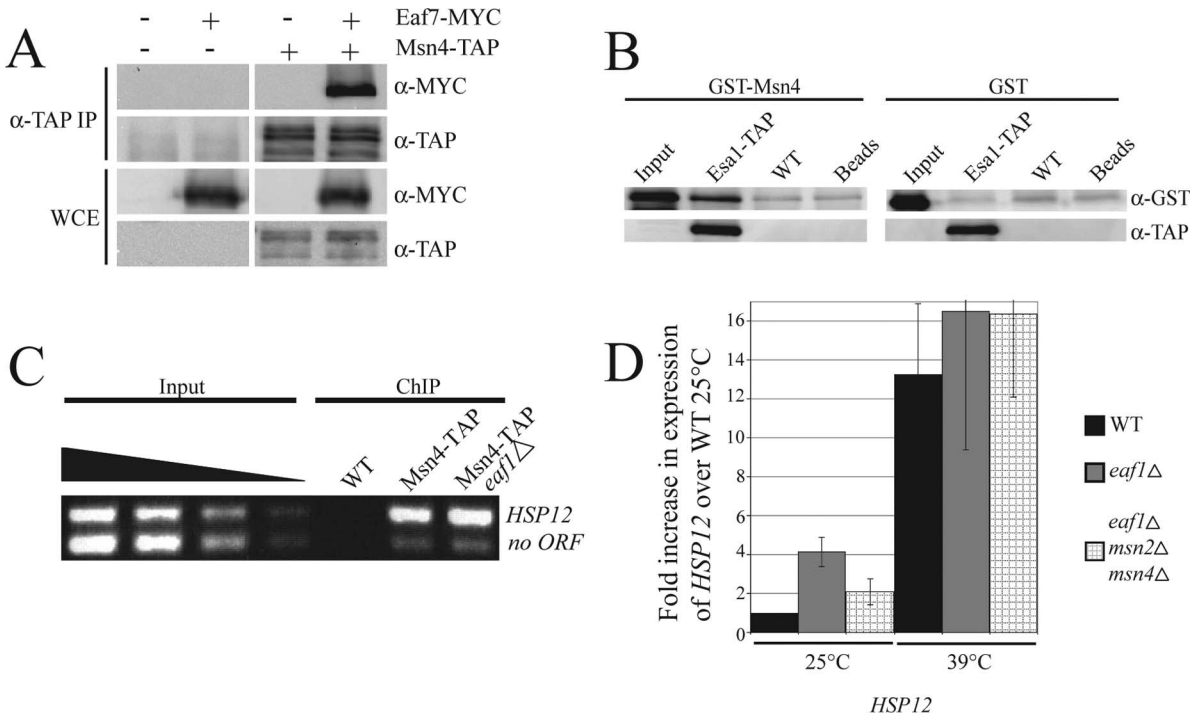

FIG. 4. NuA4 physically interacts with Msn4 but does not regulate Msn4 binding to the *HSP12* promoter or heat shock induction of *HSP12*. (A) NuA4 interacts with Msn4 in vivo. Protein extracts expressing the indicated tagged proteins (Msn4-TAP [YKB1035], Eaf7-MYC [YKB518], Msn4-TAP/Eaf7-MYC [YKB1069]) or an untagged WT control (YPH499) were immunoprecipitated with magnetic beads coated with IgG antibodies that bind the PrA component of the TAP tag. Total protein extracts (WCE) and immunoprecipitates (α-TAP IP) were resolved by 7.5% SDS-PAGE and subjected to Western blot analysis with anti-Myc and anti-TAP antibodies (α-MYC and α-TAP, respectively), as indicated at the right side of the panels. (B) NuA4 and Msn4 interact in vitro. WCE from cells expressing Esa1-TAP (YKB440) were used to purify the NuA4 complex using IgG-coated magnetic beads, and results were compared to those for an untagged strain (WT; YPH499). IgG-coated magnetic beads complexed with NuA4 (lane Esa1-TAP), background yeast proteins (lane WT), or beads alone (lane Beads) were incubated with equivalent amounts of either full-length GST-Msn4 or GST. Resulting immunocomplexes were eluted with heat, resolved by 10% SDS-PAGE, and subjected to Western blotting with anti-TAP and anti-GST antibodies, as indicated. Twenty-five percent of the input GST or GST-Msn4 fusion protein was run alongside the pull-down experiments as an input control (lane Input). (C) Msn4 occupancy at the *HSP12* promoter is independent of NuA4. Modified ChIP (see Materials and Methods) was performed using an untagged strain (WT; YPH499) and the Msn4-TAP (YKB1035) and Msn4-TAP *eaf1*Δ (YKB1091) strains. Immunoprecipitated (ChIP lanes) or WCE (Input lanes) DNA was subjected to multiplex PCR amplification using primers specific to the promoter region of *HSP12* and an intergenic region on chromosome V (*no ORF*). The results of this ChIP was representative of three experiments. (D) Deletion of *EAF1* causes derepression of *HSP12* but does not inhibit the heat shock induction of *HSP12*. WT (YPH499), *eaf1*Δ (YKB44), and *eaf1*Δ *msn2*Δ *msn4* Δ (YKB1097) cells were grown in YPD at 25°C to mid-log phase, and samples were collected at 25°C and after 30 min of heat shock treatment at 39°C. Northern blots were probed with labeled DNA fragments of the *HSP12* gene. The signal was quantitated using AlphaEase FC (Alpha Innotech) and normalized to the *ACT1* signal. The values are averages from three independent RNA preparations, and error bars indicate standard deviations.

Msn4 and/or Msn2 may bind stress response element promoters in the absence of stress and that NuA4-dependent modification of the chromatin structure may not regulate Msn2 or Msn4 binding to promoters. To test this, we examined the occupancy of Msn4 on the promoter of the *HSP12* gene by ChIP. The transcriptional induction of *HSP12* is dependent largely on Msn2/4 under stress conditions (39, 52) and is highly derepressed in NuA4 mutants in a manner dependent on Msn2/4 (37), and Esa1 has been shown to localize to the *HSP12* promoter (49). Using Msn4-TAP, we attempted a traditional ChIP experiment but found that due to the reduced accessibility of the epitope tag upon cross-linking, we were unable to immunoprecipitate Msn4-TAP. We therefore developed a modified ChIP protocol, utilizing a gentle clarification that circumvents the use of formaldehyde cross-linking, and tested for the presence of Msn4-TAP on the promoter of *HSP12*. Our modified ChIP analysis demonstrated that under normal growth conditions, Msn4-TAP associates specifically with the promoter region of *HSP12* but not with an untranscribed control region on chromosome V (Fig. 4C, row *no ORF*) (27). Through Northern blot analysis, we determined that *HSP12* is derepressed at 25°C in log-phase *eaf1*Δcells and that derepression is largely dependent on Msn2 and Msn4 (Fig. 4D). Therefore, we also performed the modified Msn4-TAP ChIP protocol with *eaf1*Δ cells and determined that the deletion of *EAF1* does not alter Msn4 localization to *HSP12* promoters (Fig. 4C). As NuA4 has been localized to the *HSP12* promoter in the absence of stress (49) and the deletion of *EAF1* causes the collapse of the NuA4 complex, the ChIP results suggest that Msn4 localization to the *HSP12* promoter does not require NuA4. We were next interested in determining whether NuA4 played a significant role in the activation of *HSP12* under heat shock conditions. To do this, we performed *HSP12* Northern blot analysis and compared WT cells to *eaf1*Δ

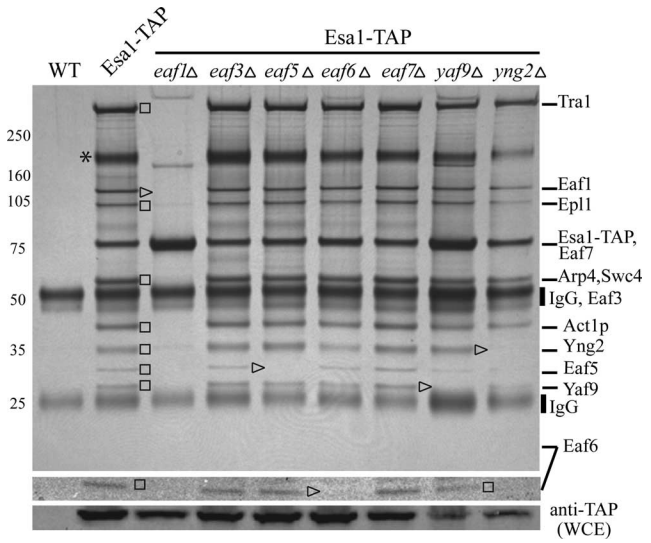

FIG. 5. Eaf1 is required for NuA4 complex integrity. SDS-PAGE (gradient gel) and silver staining of NuA4 affinity purified via Esa1-TAP (YKB440) compared to an untagged strain (WT; YPH499) and Esa1-TAP purified from mutant strain backgrounds of without all seven nonessential subunits (*eaf1*Δ [YKB855], *eaf3*Δ [YKB765], *eaf5*Δ [YKB854], *eaf6*Δ [YKB766], *eaf7*Δ [YKB964], *yaf9*Δ [YKB966], and *yng2*Δ [YKB967] strains). Eaf6, as it does not stain well with silver, was subjected to a longer exposure (middle panel). Proteins bands in the Esa1-TAP lane were identified by MS as indicated. Anti-TAP Western blotting demonstrated the expression of Esa1-TAP in the WCE of all strains tested. Arrowheads point to proteins eliminated by subunit deletion, while squares specify additional subunits lost. The * indicates a non-NuA4, copurifying protein, Fks1. Numbers at the left are molecular masses (in kDa). The gel is representative of three purification experiments.

cells after 30 min of heat shock at 39°C (Fig. 4D). The deletion of *EAF1* did not inhibit the heat shock induction of *HSP12*. This suggests that though NuA4 is important for maintaining the repression of the *HSP12* promoter, NuA4 does not play a significant role in the induction of *HSP12*. Surprisingly, we also determined that in the absence of Eaf1, the heat shock induction of *HSP12* is independent of Msn2 and Msn4 (Fig. 4D), suggesting that other transcription factors are compensating.

Eaf1 is required for NuA4 complex integrity. The large size of the *eaf1*Δ genetic-interaction profile relative to those of the other nonessential NuA4 subunits suggested that Eaf1 might have a unique and critical role in complex integrity. To test this hypothesis, we examined protein association with TAP-tagged Esa1 in cells deficient for one of the seven nonessential subunits (Fig. 5). Protein bands in the Esa1-TAP lane were identified through MS. Eaf3 comigrated with the IgG heavy chain, and Eaf7 comigrated with Esa1-TAP, so while we detected these subunits by MS in the Esa1-TAP purification, we cannot make reliable predictions as to their interactions with the complex in Esa1-TAP purifications in the various deletion mutant backgrounds. Regardless, we found that the elimination of Eaf3, Eaf5, Eaf6, Eaf7, and Yaf9 had no detectable effect on the association of the remaining visible NuA4 subunits (Fig. 5), indicating that the overall integrity of the NuA4 complex is not dependent on these subunits. Removal of Yng2 resulted in the loss of Eaf6 (Fig. 5, compare lane Esa1-TAP to lane Esa1-TAP *yng2*Δ), indicating that Eaf6 interacts with the NuA4 complex through Yng2.

Remarkably, the removal of Eaf1 resulted in a dramatic loss of NuA4 complex integrity (Fig. 5, compare lane Esa1-TAP to lane Esa1-TAP *eaf1*Δ). Though faint bands corresponding to the size of Epl1 and Yng2 were detected on the silver-stained gel as interacting with Esa1-TAP in the absence of Eaf1, no other subunits of NuA4 were detected in multiple purifications. This implies that in the absence of Eaf1, Piccolo NuA4, which is sufficient for cellular viability (7), is still present. These results suggest that Eaf1 is required to maintain the integrity of the NuA4 complex and may link the Piccolo NuA4 subcomplex to the remaining NuA4 components.

Eaf5 and Eaf7 form a subcomplex. We were surprised that the deletion of most nonessential subunits revealed little about the physical interdependencies of the NuA4 subunits within the complex. As genes that function within the same complex or subcomplex tend to have similar genetic-interaction profiles, to gain further insight into NuA4 complex integrity, we performed two-dimensional hierarchical clustering of our NuA4 genetic interactions (Fig. 6A). Our analysis revealed that *EAF5*, *EAF7*, and *EAF3* components cluster together. We also performed a two-dimensional hierarchical clustering analysis of our NuA4 genetic interactions in the context of a large combined data set consisting of 12,954 previously published SL or SS interactions that were identified using genome-wide SL-SGA screens (supplementary cluster Treeview files are available at www.oisb.ca/personal_web_site/Baetz_Lab/publicationsFS.html) (40, 45, 48, 64). This analysis further confirmed the idea that *EAF3*, *EAF5*, and *EAF7* cluster together. Similar clustering of *EAF5* and *EAF7* was seen in the recently published chromatin E-MAPs (14), and *eaf5*Δ and *eaf7*Δ strains display similarity in microarray transcriptional profiles (31). The repeated clustering of *EAF5*, *EAF7*, and *EAF3* genetic profiles strongly suggests that Eaf5, Eaf7, and potentially Eaf3 may form a subcomplex that is responsible for mediating only a subset of the cellular functions of NuA4. We have shown that the interaction of Eaf5 with the NuA4 complex is not dependent on Eaf7 (Fig. 5); however, as Eaf7 was not visible on the silver-stained gel, we could not visually determine whether Eaf5 is required for Eaf7's interaction with NuA4. Therefore, to further investigate the possible existence of this subcomplex, we chose to integrate a C-terminal Myc tag at the *EAF7* chromosomal locus in order to determine the effect of *EAF5* gene deletion on the Eaf7-Myc interaction with the NuA4 complex by Western blotting. We purified the NuA4 complex using Esa1-TAP and found that the *eaf5*Δ mutant disrupted the interaction of Eaf7-Myc with the NuA4 complex (Fig. 6B). We were next interested in determining whether Eaf7 and Eaf5 form a detectable subcomplex in the absence of NuA4. To explore this, we TAP tagged Eaf7 and studied whether the Eaf5-Eaf7 subcomplex would still form in the absence of Eaf1, which eliminates the full NuA4 complex. We found that while all of the other NuA4 subunits were lost as a result of the Eaf1 deletion, the physical interaction of Eaf7 with Eaf5 remained intact (Fig. 6C). Taken together, these results indicate the presence of a novel subcomplex forming between Eaf5 and Eaf7 within the NuA4 complex and, moreover, that Eaf7 interacts with NuA4 through Eaf5.

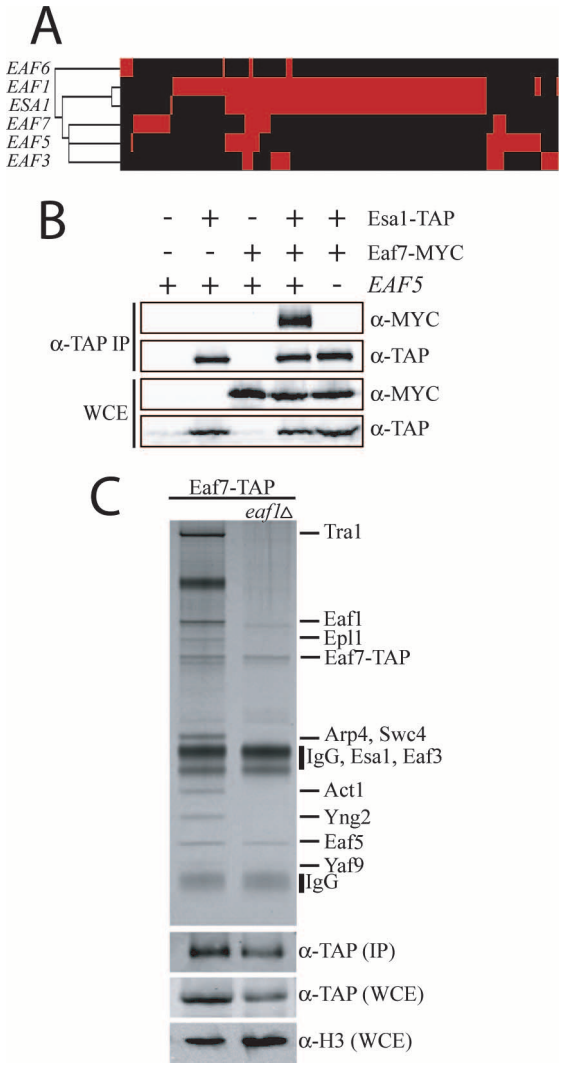

FIG. 6. Eaf5 and Eaf7 form a subcomplex within NuA4. (A) Two-dimensional, hierarchical clustering of the NuA4 synthetic genetic interactions. Rows display NuA4 query genes, columns indicate the interacting deletion mutant array genes, and a red box indicates genetic interaction. The cluster includes genetic interactions for the *esa1*(L245P) mutant that were directly tested against all *eaf1*Δ genetic interactions. (B) Eaf7 interacts with NuA4 through Eaf5. Shown are results with protein extracts prepared from strains expressing the indicated tagged proteins (Esa1-TAP [YKB440], Eaf7-Myc [YKB518], Esa1-TAP Eaf7-Myc [YKB1054], and Esa1-TAP Eaf7-Myc *eaf5*Δ [YKB1043]) or an untagged WT (YPH499); immunoprecipitations were performed using magnetic beads coated with IgG antibodies that bind the PrA component of the TAP tag. Total protein extracts (WCE) and anti-TAP immunoprecipitates (IP) were then resolved by 7.5% SDS-PAGE and subjected to Western blot analysis with anti-Myc and anti-TAP antibodies, as indicated on the right side of the panels. α, anti. (C) Eaf7 and Eaf5 form a subcomplex in the absence of Eaf1. SDS-PAGE (gradient gel) and silver staining of NuA4 affinity purified with Eaf7-TAP in the presence (YKB442) and absence (*eaf1*Δ) of Eaf1 (YKB1034). Anti-TAP Western blotting was carried out on WCE as well as on 10% of the IP eluate. An anti-histone H3 (α-H3) Western blot analysis of WCE demonstrates equal protein loadings. The results are representative of three purification experiments.

DISCUSSION

NuA4 is a genetic hub. In an effort to further define the cellular functions of NuA4 and provide insight into the function of individual NuA4 subunits, we performed genome-wide SL-SGA analysis with five nonessential subunits of NuA4. With the inclusion of previously confirmed genetic interactions, the combined data set contains 268 genetic interactions among 204 genes (Fig. 1). The most remarkable feature of the genetic-interaction map is that the *eaf1*Δ query mutant accounted for 148 genetic interactions alone, which is more than four times greater than the average number of interactions per query mutant in other genome-wide screens (64). Further, the genes identified by the *eaf1*Δ mutant were not limited to genes with roles in chromatin biology previously linked to NuA4; rather, the genetic interaction profile for the *eaf1*Δ mutant indicates new and diverse functional relationships for NuA4, such as protein transport, arginine biosynthesis, stress response, and ubiquitination (Fig. 1A). Though it is possible that Eaf1 has cellular functions outside NuA4, the lack of additional protein interactions (Fig. 2) and the high degree of overlap in genetic-interaction profiles between *eaf1*Δ and *esa1*(*L245P*) cells (Fig. 6A; see Supplemental Table 2 at www.oisb.ca/personal_web_site/Baetz_Lab/publicationsFS.html) strongly suggest that the sole function of Eaf1 is as a component of NuA4. Of the few *eaf1*Δ mutant genetic interactions that were not shared with *esa1*(*L245P*), it is possible that the interactions occur at higher temperatures or with other *esa1* alleles. As Esa1 is essential and part of Piccolo NuA4, *esa1* mutants will likely display numerous genetic interactions distinct from that of the *eaf1*Δ mutant. Regardless, the large number of interactions identified for both *eaf1* and *esa1*(*L245P*) indicates that these are "hub genes" (64).

It has been hypothesized that highly connected genetic-hub genes are more important for cellular fitness, are more likely to encode essential genes, and are highly conserved across species (15, 35, 64). Genetic-hub genes may act as genetic buffers because the loss of hub genes causes in enhancement of mutant phenotypes in otherwise unconnected, diverse cellular functions. This may explain the identification of seemingly disparate genes in the *eaf1*Δ SL-SGA screen. Recently, systematic mapping of genetic interactions in *C. elegans* identified numerous genes encoding chromatin-modifying proteins as genetic hubs, including *mys-1* and *trr-1*, the orthologs of *ESA1* and *TRA1*, respectively (35). This indicates that NuA4/Tip60 mutants likely act as genetic hubs across species.

How might NuA4 and other chromatin modifiers act as global genetic buffers? The most likely scenario is that a loss of function of NuA4 leads to global changes in acetylation patterns of histones, which subsequently affects transcription. NuA4 mutants alone display relatively minor effects on global transcriptional profiles, as detected in microarray studies (11, 19, 27, 31, 36, 69). However, these transcriptional deficiencies in combination with other mutant genes may result in a dramatic enhancement of phenotypes or fitness defects. For example, we determined that nonessential NuA4 mutants display SS or SL interactions with mutant genes encoding proteins required for arginine biosynthesis (Fig. 1). Microarray studies have shown that NuA4 mutants display modest two- to threefold decreases in the transcription of numerous genes in the

arginine biosynthesis pathway (11, 19, 31, 36). While the deletion of single genes of this pathway does not result in fitness defects, we suspect that this deletion in combination with decreases in the NuA4-dependent transcription of arginine pathway genes results in fitness defects. Moreover, we hypothesize that NuA4 buffers the effects of the vesicle-mediated transport mutants in a similar manner. Microarray studies of NuA4 or *htz1*Δ mutants (11, 19, 27, 30, 31, 36, 41, 42, 69) provide no insights into the transcriptional misregulation of the key gene(s) required for vesicle-mediated transport. However, as *htz1*Δ cells display genetic interactions and vacuolar morphological defects similar to those of *eaf1*Δ and *esa1*(*L245P*) cells (Fig. 3), we favor a model where NuA4's and Htz1's roles as genetic buffers are through transcriptional effects. As *htz1-ND* mutants do not display vacuolar morphological defects, it is likely that NuA4's transcriptional effects are not mediated through Htz1 N-terminal tail acetylation but rather through H4 acetylation or alternative targets. Further, numerous strains containing deletions of NuA4, SWR complex, and *HTZ1* genes were identified in a high-throughput screen aimed at identifying diploid, homozygous deletion mutants with carboxypeptidase Y vacuolar sorting defects (6).

Genetic hubs are thought to be major contributors to complex genetic diseases arising from multiple mutations (reviewed in reference 9). Mutations in genetic hubs may modify the effects of numerous mutations, resulting in the implication of genetic hub genes in a diverse range of apparently unrelated diseases. As mutant components of NuA4/Tip60s in both yeast and *C. elegans* act as genetic hubs, it is likely that this trait is shared with human Tip60. If Tip60 is a genetic hub, it would explain the connection of Tip60 with pleiotropic roles in a diverse range of cancers, neurodegenerative diseases, and viral infections (51). Insights derived from the NuA4 genetic map presented in this paper, along with extension of the map using mutant alleles of essential NuA4 genes, will provide an excellent source of testable hypotheses for determining the exact molecular mechanisms through which Tip60 may contribute to clinical pathology.

NuA4 as a transcriptional repressor of stress response genes. Traditionally, it has been proposed that HAT acetylation of histones is correlated with transcriptional activation but that HDAC deacetylation of histones is correlated with transcriptional repression (reviewed in reference 33). While NuA4 is required for transcriptional activation, growing evidence indicates that NuA4 also has a role in the transcriptional repression of a subset of Msn2/4-dependent stress-responsive genes, including *HSP12* (Fig. 4D) (25, 37). In our study, the identification of 10 genes involved in stress response in the NuA4 SL-SGA screen (Fig. 1) and the identification of a physical interaction between Msn4 and NuA4 (Fig. 4A and B) further support the role of NuA4 in stress response.

How might NuA4 repress the Msn2/4-dependent transcription of stress response genes? Microarray studies indicate that derepression of the subset of Msn2/4-dependent genes also occurs in *HTZ1* deletion mutants (41, 43) and histone H4 mutants defective in N-terminal acetylation (16), suggesting that NuA4 could mediate the repression of these genes through the acetylation of these two histones. We do not believe that NuA4 acetylation of histones inhibits the access of Msn2 and/or Msn4 to stress-dependent promoters, as we reproducibly detect Msn4 occupancy at the *HSP12* promoter under nonstress conditions and moreover show that the deletion of *EAF1* does not result in increased Msn4 localization to this promoter (Fig. 4C). Though it is possible that the localization of Msn4 to *HSP12* promoters is dependent on Piccolo NuA4, which appears to be present in an *eaf1*Δ strain, we believe that this is unlikely, as there is presently no evidence of targeted Piccolo NuA4 activity. Alternatively, the physical interaction between Msn2/4 and NuA4 may target NuA4 histone acetylation to promoters to promote a repressed chromatin state through the recruitment of chromatin remodelers or repressors. Despite multiple ChIP attempts, we were not able to reproducibly determine whether or not Esa1-TAP localization to the *HSP12* promoter is changed in *msn2*Δ *msn4*Δ strains. NuA4 may also directly acetylate Msn4 or Msn2, thereby masking activation domains or regulating additional protein interactions required for the activation or repression of Msn2/4-dependent genes. This may explain the role of the physical interactions seen between NuA4 and Msn2 and/or Msn4. Surprisingly, though *HSP12* heat shock induction has been shown to be largely dependent on Msn2/4, in *eaf1*Δ *msn2*Δ *msn4*Δ cells, *HSP12* is still induced upon heat shock (Fig. 4D). This suggests that alternative transcription factors, such as Hsf1 (49), may play a significant role in the absence of NuA4. Unraveling the mysteries of the molecular function of NuA4 in Msn2/4-dependent gene repression will require further in-depth study.

NuA4 complex structure and function. Though it has been proposed that genes encoding proteins in the same pathway or complex should have similar synthetic genetic interactions, a surprising feature of our NuA4 genetic map was the dramatic difference in the numbers of interactions for components and in some cases the lack of overlap between the queries. As genetic interactions that were identified in one screen were not directly tested against all the queries, some of the lack of overlap may be explained by the inherent rate of false-negative results of SL-SGA screening. In the case of the *eaf3*Δ and *eaf6*Δ screens, some of the unique genetic interactions may be the result of the Eaf3 and Eaf6 proteins also being part of the Rpd3S and NuA3 complexes, respectively (10, 27, 60). However, in the case of the *eaf1*Δ mutant, the striking number of genetic interactions displayed is likely reflective of the role that Eaf1 plays in NuA4 complex integrity. We determined that in the absence of Eaf1, the full NuA4 complex collapses (Fig. 5 and 6). Despite the dramatic effect on NuA4 complex integrity, *EAF1* is not an essential gene. This is likely a reflection of the fact that in the absence of Eaf1, Piccolo NuA4 is still detected (Fig. 5). Piccolo NuA4 contains the only two essential NuA4 proteins, Esa1 and Epl1, that are exclusively found in NuA4, and as previously suggested, Piccolo NuA4 likely mediates the essential nontargeted global acetylation of the histones of NuA4 (7). However, with Eaf1 being a scaffold protein, the diverse genetic interactions identified in the *eaf1*Δ screen may reflect the sum of the proposed recruitment roles of the remaining 10 non-Piccolo NuA4 subunits. Alternatively, Eaf1 may perform unique recruitment or regulatory roles that are not shared with the other nine subunits.

The clustering of our genome-wide NuA4 genetic interactions (Fig. 6A; supplementary cluster Treeview files are available at www.oisb.ca/personal_web_site/Baetz_Lab/publicationsFS

.html) and the chromatin E-MAP (14) allowed us to make predictions regarding a possible subcomplex involving Eaf5 and Eaf7. We confirmed that Eaf5 and Eaf7 form a subcomplex and that Eaf7 interacts with the NuA4 complex through Eaf5 (Fig. 6B and C). The genetic network also predicts that Eaf3 may be a component of this subcomplex. Work from Jacques Coté's laboratory has confirmed an Eaf3 -Eaf5-Eaf7 subcomplex (personal communication). Though we presently do not know if the subcomplex is purely structural in nature, it is likely that it mediates a distinct set of NuA4 cellular functions. As the majority of the genetic interactions shared between the *eaf3*Δ, *eaf5*Δ, and *eaf7*Δ mutants are with SWR complex mutants or the *htz1*Δ mutant, this suggests that the subcomplex performs a function distinct from NuA4's role in Htz1 acetylation. This idea is further solidified by the fact that *eaf3*Δ, *eaf5*Δ, and *eaf7*Δ mutants do not display mutant phenotypes that are shared with SWR complex, *HTZ1*, and other NuA4 mutants implicated in Htz1 acetylation. For example, *eaf3*Δ, *eaf5*Δ, and *eaf7*Δ mutants display either no or only modest increases in chromosome segregation defects (31) (data not shown), are not sensitive to benomyl (31), are not defective in Htz1 K14 acetylation (28), and do not display defects in vacuole morphology as detected with FM4-64 (Fig. 3A). As *eaf5*Δ and *eaf7*Δ mutants have similar effects on gene expression (31), it is likely that the Eaf3-Eaf5-Eaf7 subcomplex is required for a distinct subset of NuA4 cellular functions, possibly through the recruitment of NuA4 to distinct chromatin loci.

Our work indicates that genome-wide genetic interaction maps not only provide valuable insights into query gene function and complex composition but also may be extremely useful in discerning structural integrity and subcomplexes of large, multisubunit protein complexes. It will be interesting to see whether additional SGA screens using mutants with point or domain mutations in NuA4 genes that specifically abolish protein interactions will provide greater insight into the function of each NuA4 subunit.

ACKNOWLEDGMENTS

We thank M. C. Keogh, J. Dillingham, and J. Greenblatt for providing yeast strains; M. C. Keogh, V. Measday, and members of the Baetz laboratory for helpful discussion and critical reading of the manuscript; A. Rudner and M. C. Keogh for technical support; and J. Coté for communicating results prior to publication.

This work was supported by operating grants from the National Cancer Institute of Canada through funds raised by the Terry Fox Research Foundation and an Early Research Award from the Ontario Government (to K.B.). Funding was also received from the Canada Foundation for Innovation, Natural Sciences and Engineering Research Council of Canada; the Canadian Institute of Health Research (CIHR); the Heart and Stroke Foundation of Ontario Centre for Stroke Recovery; La Fondation Jean-Louis Lévesque; and the Ontario Government (to D.F.). K.B. is a Canada Research Chair in Chemical and Functional Genomics. D.F. is a Canada Research Chair in Proteomics and Systems Biology. L.M was supported by an Ontario Graduate Student Award and a CIHR Doctoral Award. J.-P.L was supported by an Ontario Graduate Student Award. I.S.S. was supported by a Canadian Institute of Aging Investigator Award. A.S.A.-M. was supported by an Ontario Women's Health Council/CIHR Institute of Gender and Health Fellowship.

REFERENCES

1. **Allard, S., R. T. Utley, J. Savard, A. Clarke, P. Grant, C. J. Brandl, L. Pillus, J. L. Workman, and J. Cote.** 1999. NuA4, an essential transcription adaptor/histone H4 acetyltransferase complex containing Esa1p and the ATM-related cofactor Tra1p. EMBO J. **18:**5108–5119.
2. **Babiarz, J. E., J. E. Halley, and J. Rine.** 2006. Telomeric heterochromatin boundaries require NuA4-dependent acetylation of histone variant H2A.Z in Saccharomyces cerevisiae. Genes Dev. **20:**700–710.
3. **Baetz, K., J. Moffat, J. Haynes, M. Chang, and B. Andrews.** 2001. Transcriptional coregulation by the cell integrity mitogen-activated protein kinase Slt2 and the cell cycle regulator Swi4. Mol. Cell. Biol. **21:**6515–6528.
4. **Bird, A. W., D. Y. Yu, M. G. Pray-Grant, Q. Qiu, K. E. Harmon, P. C. Megee, P. A. Grant, M. M. Smith, and M. F. Christman.** 2002. Acetylation of histone H4 by Esa1 is required for DNA double-strand break repair. Nature **419:**411–415.
5. **Bittner, C. B., D. T. Zeisig, B. B. Zeisig, and R. K. Slany.** 2004. Direct physical and functional interaction of the NuA4 complex components Yaf9p and Swc4p. Eukaryot. Cell **3:**976–983.
6. **Bonangelino, C. J., E. M. Chavez, and J. S. Bonifacino.** 2002. Genomic screen for vacuolar protein sorting genes in Saccharomyces cerevisiae. Mol. Biol. Cell **13:**2486–2501.
7. **Boudreault, A. A., D. Cronier, W. Selleck, N. Lacoste, R. T. Utley, S. Allard, J. Savard, W. S. Lane, S. Tan, and J. Cote.** 2003. Yeast enhancer of polycomb defines global Esa1-dependent acetylation of chromatin. Genes Dev. **17:**1415–1428.
8. **Brown, C. E., L. Howe, K. Sousa, S. C. Alley, M. J. Carrozza, S. Tan, and J. L. Workman.** 2001. Recruitment of HAT complexes by direct activator interactions with the ATM-related Tra1 subunit. Science **292:**2333–2337.
9. **Bussey, H., B. Andrews, and C. Boone.** 2006. From worm genetic networks to complex human diseases. Nat. Genet. **38:**862–863.
10. **Carrozza, M. J., B. Li, L. Florens, T. Suganuma, S. K. Swanson, K. K. Lee, W. J. Shia, S. Anderson, J. Yates, M. P. Washburn, and J. L. Workman.** 2005. Histone H3 methylation by Set2 directs deacetylation of coding regions by Rpd3S to suppress spurious intragenic transcription. Cell **123:**581–592.
11. **Choy, J. S., and S. J. Kron.** 2002. NuA4 subunit Yng2 function in intra-S-phase DNA damage response. Mol. Cell. Biol. **22:**8215–8225.
12. **Choy, J. S., B. T. Tobe, J. H. Huh, and S. J. Kron.** 2001. Yng2p-dependent NuA4 histone H4 acetylation activity is required for mitotic and meiotic progression. J. Biol. Chem. **276:**43653–43662.
13. **Clarke, A. S., J. E. Lowell, S. J. Jacobson, and L. Pillus.** 1999. Esa1p is an essential histone acetyltransferase required for cell cycle progression. Mol. Cell. Biol. **19:**2515–2526.
14. **Collins, S. R., K. M. Miller, N. L. Maas, A. Roguev, J. Fillingham, C. S. Chu, M. Schuldiner, M. Gebbia, J. Recht, M. Shales, H. Ding, H. Xu, J. Han, K. Ingvarsdottir, B. Cheng, B. Andrews, C. Boone, S. L. Berger, P. Hieter, Z. Zhang, G. W. Brown, C. J. Ingles, A. Emili, C. D. Allis, D. P. Toczyski, J. S. Weissman, J. F. Greenblatt, and N. J. Krogan.** 2007. Functional dissection of protein complexes involved in yeast chromosome biology using a genetic interaction map. Nature **446:**806–810.
15. **Davierwala, A. P., J. Haynes, Z. Li, R. L. Brost, M. D. Robinson, L. Yu, S. Mnaimneh, H. Ding, H. Zhu, Y. Chen, X. Cheng, G. W. Brown, C. Boone, B. J. Andrews, and T. R. Hughes.** 2005. The synthetic genetic interaction spectrum of essential genes. Nat. Genet. **37:**1147–1152.
16. **Dion, M. F., S. J. Altschuler, L. F. Wu, and O. J. Rando.** 2005. Genomic characterization reveals a simple histone H4 acetylation code. Proc. Natl. Acad. Sci. USA **102:**5501–5506.
17. **Downs, J. A., S. Allard, O. Jobin-Robitaille, A. Javaheri, A. Auger, N. Bouchard, S. J. Kron, S. P. Jackson, and J. Cote.** 2004. Binding of chromatin-modifying activities to phosphorylated histone H2A at DNA damage sites. Mol. Cell **16:**979–990.
18. **Doyon, Y., and J. Cote.** 2004. The highly conserved and multifunctional NuA4 HAT complex. Curr. Opin. Genet. Dev. **14:**147–154.
19. **Durant, M., and B. F. Pugh.** 2006. Genome-wide relationships between TAF1 and histone acetyltransferases in *Saccharomyces cerevisiae*. Mol. Cell. Biol. **26:**2791–2802.
20. **Eberharter, A., S. John, P. A. Grant, R. T. Utley, and J. L. Workman.** 1998. Identification and analysis of yeast nucleosomal histone acetyltransferase complexes. Methods **15:**315–321.
21. **Eisen, A., R. T. Utley, A. Nourani, S. Allard, P. Schmidt, W. S. Lane, J. C. Lucchesi, and J. Cote.** 2001. The yeast NuA4 and Drosophila MSL complexes contain homologous subunits important for transcription regulation. J. Biol. Chem. **276:**3484–3491.
22. **Gavin, A. C., P. Aloy, P. Grandi, R. Krause, M. Boesche, M. Marzioch, C. Rau, L. J. Jensen, S. Bastuck, B. Dumpelfeld, A. Edelmann, M. A. Heurtier, V. Hoffman, C. Hoefert, K. Klein, M. Hudak, A. M. Michon, M. Schelder, M. Schirle, M. Remor, T. Rudi, S. Hooper, A. Bauer, T. Bouwmeester, G. Casari, G. Drewes, G. Neubauer, J. M. Rick, B. Kuster, P. Bork, R. B. Russell, and G. Superti-Furga.** 2006. Proteome survey reveals modularity of the yeast cell machinery. Nature **440:**631–636.
23. **Glozak, M. A., N. Sengupta, X. Zhang, and E. Seto.** 2005. Acetylation and deacetylation of non-histone proteins. Gene **363:**15–23.
24. **Gorner, W., E. Durchschlag, M. T. Martinez-Pastor, F. Estruch, G. Ammerer, B. Hamilton, H. Ruis, and C. Schuller.** 1998. Nuclear localization of the C2H2 zinc finger protein Msn2p is regulated by stress and protein kinase A activity. Genes Dev. **12:**586–597.

25. **Gorzer, I., C. Schuller, E. Heidenreich, L. Krupanska, K. Kuchler, and U. Wintersberger.** 2003. The nuclear actin-related protein Act3p/Arp4p of Saccharomyces cerevisiae is involved in transcription regulation of stress genes. Mol. Microbiol. **50:**1155–1171.
26. **Jahn, R., and R. H. Scheller.** 2006. SNAREs—engines for membrane fusion. Nat. Rev. Mol. Cell Biol. **7:**631–643.
27. **Keogh, M. C., S. K. Kurdistani, S. A. Morris, S. H. Ahn, V. Podolny, S. R. Collins, M. Schuldiner, K. Chin, T. Punna, N. J. Thompson, C. Boone, A. Emili, J. S. Weissman, T. R. Hughes, B. D. Strahl, M. Grunstein, J. F. Greenblatt, S. Buratowski, and N. J. Krogan.** 2005. Cotranscriptional set2 methylation of histone H3 lysine 36 recruits a repressive Rpd3 complex. Cell **123:**593–605.
28. **Keogh, M. C., T. A. Mennella, C. Sawa, S. Berthelet, N. J. Krogan, A. Wolek, V. Podolny, L. R. Carpenter, J. F. Greenblatt, K. Baetz, and S. Buratowski.** 2006. The Saccharomyces cerevisiae histone H2A variant Htz1 is acetylated by NuA4. Genes Dev. **20:**660–665.
29. **Klis, F. M., P. Mol, K. Hellingwerf, and S. Brul.** 2002. Dynamics of cell wall structure in Saccharomyces cerevisiae. FEMS Microbiol. Rev. **26:**239–256.
30. **Kobor, M. S., S. Venkatasubrahmanyam, M. D. Meneghini, J. W. Gin, J. L. Jennings, A. J. Link, H. D. Madhani, and J. Rine.** 2004. A protein complex containing the conserved Swi2/Snf2-related ATPase Swr1p deposits histone variant H2A.Z into euchromatin. PLoS Biol. **2:**E131.
31. **Krogan, N. J., K. Baetz, M. C. Keogh, N. Datta, C. Sawa, T. C. Kwok, N. J. Thompson, M. G. Davey, J. Pootoolal, T. R. Hughes, A. Emili, S. Buratowski, P. Hieter, and J. F. Greenblatt.** 2004. Regulation of chromosome stability by the histone H2A variant Htz1, the Swr1 chromatin remodeling complex, and the histone acetyltransferase NuA4. Proc. Natl. Acad. Sci. USA **101:**13513–13518.
32. **Krogan, N. J., G. Cagney, H. Yu, G. Zhong, X. Guo, A. Ignatchenko, J. Li, S. Pu, N. Datta, A. P. Tikuisis, T. Punna, J. M. Peregrin-Alvarez, M. Shales, X. Zhang, M. Davey, M. D. Robinson, A. Paccanaro, J. E. Bray, A. Sheung, B. Beattie, D. P. Richards, V. Canadien, A. Lalev, F. Mena, P. Wong, A. Starostine, M. M. Canete, J. Vlasblom, S. Wu, C. Orsi, S. R. Collins, S. Chandran, R. Haw, J. J. Rilstone, K. Gandi, N. J. Thompson, G. Musso, P. St. Onge, S. Ghanny, M. H. Lam, G. Butland, A. M. Altaf-Ul, S. Kanaya, A. Shilatifard, E. O'Shea, J. S. Weissman, C. J. Ingles, T. R. Hughes, J. Parkinson, M. Gerstein, S. J. Wodak, A. Emili, and J. F. Greenblatt.** 2006. Global landscape of protein complexes in the yeast Saccharomyces cerevisiae. Nature **440:**637–643.
33. **Kurdistani, S. K., and M. Grunstein.** 2003. Histone acetylation and deacetylation in yeast. Nat. Rev. Mol. Cell Biol. **4:**276–284.
34. **Lee, K. K., and J. L. Workman.** 2007. Histone acetyltransferase complexes: one size doesn't fit all. Nat. Rev. Mol. Cell Biol. **8:**284–295.
35. **Lehner, B., C. Crombie, J. Tischler, A. Fortunato, and A. G. Fraser.** 2006. Systematic mapping of genetic interactions in Caenorhabditis elegans identifies common modifiers of diverse signaling pathways. Nat. Genet. **38:**896–903.
36. **Le Masson, I., D. Y. Yu, K. Jensen, A. Chevalier, R. Courbeyrette, Y. Boulard, M. M. Smith, and C. Mann.** 2003. Yaf9, a novel NuA4 histone acetyltransferase subunit, is required for the cellular response to spindle stress in yeast. Mol. Cell. Biol. **23:**6086–6102.
37. **Lindstrom, K. C., J. C. Vary, Jr., M. R. Parthun, J. Delrow, and T. Tsukiyama.** 2006. Isw1 functions in parallel with the NuA4 and Swr1 complexes in stress-induced gene repression. Mol. Cell. Biol. **26:**6117–6129.
38. **Longtine, M. S., A. McKenzie III, D. J. Demarini, N. G. Shah, A. Wach, A. Brachat, P. Philippsen, and J. R. Pringle.** 1998. Additional modules for versatile and economical PCR-based gene deletion and modification in Saccharomyces cerevisiae. Yeast **14:**953–961.
39. **Martinez-Pastor, M. T., G. Marchler, C. Schuller, A. Marchler-Bauer, H. Ruis, and F. Estruch.** 1996. The Saccharomyces cerevisiae zinc finger proteins Msn2p and Msn4p are required for transcriptional induction through the stress response element (STRE). EMBO J. **15:**2227–2235.
40. **Measday, V., K. Baetz, J. Guzzo, K. Yuen, T. Kwok, B. Sheikh, H. Ding, R. Ueta, T. Hoac, B. Cheng, I. Pot, A. Tong, Y. Yamaguchi-Iwai, C. Boone, P. Hieter, and B. Andrews.** 2005. Systematic yeast synthetic lethal and synthetic dosage lethal screens identify genes required for chromosome segregation. Proc. Natl. Acad. Sci. USA **102:**13956–13961.
41. **Meneghini, M. D., M. Wu, and H. D. Madhani.** 2003. Conserved histone variant H2A.Z protects euchromatin from the ectopic spread of silent heterochromatin. Cell **112:**725–736.
42. **Millar, C. B., F. Xu, K. Zhang, and M. Grunstein.** 2006. Acetylation of H2AZ Lys 14 is associated with genome-wide gene activity in yeast. Genes Dev. **20:**711–722.
43. **Mizuguchi, G., X. Shen, J. Landry, W. H. Wu, S. Sen, and C. Wu.** 2004. ATP-driven exchange of histone H2AZ variant catalyzed by SWR1 chromatin remodeling complex. Science **303:**343–348.
44. **Oka, T., and M. Krieger.** 2005. Multi-component protein complexes and Golgi membrane trafficking. J. Biochem. (Tokyo) **137:**109–114.
45. **Pan, X., P. Ye, D. S. Yuan, X. Wang, J. S. Bader, and J. D. Boeke.** 2006. A DNA integrity network in the yeast Saccharomyces cerevisiae. Cell **124:**1069–1081.
46. **Pfeffer, S., and D. Aivazian.** 2004. Targeting Rab GTPases to distinct membrane compartments. Nat. Rev. Mol. Cell Biol. **5:**886–896.
47. **Puig, O., F. Caspary, G. Rigaut, B. Rutz, E. Bouveret, E. Bragado-Nilsson, M. Wilm, and B. Seraphin.** 2001. The tandem affinity purification (TAP) method: a general procedure of protein complex purification. Methods **24:**218–229.
48. **Reguly, T., A. Breitkreutz, L. Boucher, B. J. Breitkreutz, G. C. Hon, C. L. Myers, A. Parsons, H. Friesen, R. Oughtred, A. Tong, C. Stark, Y. Ho, D. Botstein, B. Andrews, C. Boone, O. G. Troyanskya, T. Ideker, K. Dolinski, N. N. Batada, and M. Tyers.** 2006. Comprehensive curation and analysis of global interaction networks in Saccharomyces cerevisiae. J. Biol. **5:**11.
49. **Reid, J. L., V. R. Iyer, P. O. Brown, and K. Struhl.** 2000. Coordinate regulation of yeast ribosomal protein genes is associated with targeted recruitment of Esa1 histone acetylase. Mol. Cell **6:**1297–1307.
50. **Sanchez, C., I. Sanchez, J. A. Demmers, P. Rodriguez, J. Strouboulis, and M. Vidal.** 2007. Proteomics analysis of Ring1B/Rnf2 interactors identifies a novel complex with the Fbxl10/Jhdm1B histone demethylase and the Bcl6 interacting corepressor. Mol. Cell. Proteomics **6:**820–834.
51. **Sapountzi, V., I. R. Logan, and C. N. Robson.** 2006. Cellular functions of TIP60. Int. J. Biochem. Cell. Biol. **38:**1496–1509.
52. **Schmitt, A. P., and K. McEntee.** 1996. Msn2p, a zinc finger DNA-binding protein, is the transcriptional activator of the multistress response in Saccharomyces cerevisiae. Proc. Natl. Acad. Sci. USA **93:**5777–5782.
53. **Schmitt, M. E., T. A. Brown, and B. L. Trumpower.** 1990. A rapid and simple method for preparation of RNA from Saccharomyces cerevisiae. Nucleic Acids Res. **18:**3091–3092.
54. **Seeley, E. S., M. Kato, N. Margolis, W. Wickner, and G. Eitzen.** 2002. Genomic analysis of homotypic vacuole fusion. Mol. Biol. Cell **13:**782–794.
55. **Selleck, W., I. Fortin, D. Sermwittayawong, J. Cote, and S. Tan.** 2005. The *Saccharomyces cerevisiae* Piccolo NuA4 histone acetyltransferase complex requires the Enhancer of Polycomb A domain and chromodomain to acetylate nucleosomes. Mol. Cell. Biol. **25:**5535–5542.
56. **Shevchenko, A., O. N. Jensen, A. V. Podtelejnikov, F. Sagliocco, M. Wilm, O. Vorm, P. Mortensen, A. Shevchenko, H. Boucherie, and M. Mann.** 1996. Linking genome and proteome by mass spectrometry: large-scale identification of yeast proteins from two dimensional gels. Proc. Natl. Acad. Sci. USA **93:**14440–14445.
57. **Sikorski, R. S., and P. Hieter.** 1989. A system of shuttle vectors and yeast host strains designed for efficient manipulation of DNA in Saccharomyces cerevisiae. Genetics **122:**19–27.
58. **Smith, E. R., A. Eisen, W. Gu, M. Sattah, A. Pannuti, J. Zhou, R. G. Cook, J. C. Lucchesi, and C. D. Allis.** 1998. ESA1 is a histone acetyltransferase that is essential for growth in yeast. Proc. Natl. Acad. Sci. USA **95:**3561–3565.
59. **Squatrito, M., C. Gorrini, and B. Amati.** 2006. Tip60 in DNA damage response and growth control: many tricks in one HAT. Trends Cell Biol. **16:**433–442.
60. **Taverna, S. D., S. Ilin, R. S. Rogers, J. C. Tanny, H. Lavender, H. Li, L. Baker, J. Boyle, L. P. Blair, B. T. Chait, D. J. Patel, J. D. Aitchison, A. J. Tackett, and C. D. Allis.** 2006. Yng1 PHD finger binding to H3 trimethylated at K4 promotes NuA3 HAT activity at K14 of H3 and transcription at a subset of targeted ORFs. Mol. Cell **24:**785–796.
61. **Thomas, T., and A. K. Voss.** 2007. The diverse biological roles of MYST histone acetyltransferase family proteins. Cell Cycle **6:**696–704.
62. **Tong, A., and C. Boone.** 2006. Synthetic genetic array (SGA) analysis in Saccharomyces cerevisiae. Methods Mol. Biol. **313:**171–192.
63. **Tong, A. H., M. Evangelista, A. B. Parsons, H. Xu, G. D. Bader, N. Page, M. Robinson, S. Raghibizadeh, C. W. Hogue, H. Bussey, B. Andrews, M. Tyers, and C. Boone.** 2001. Systematic genetic analysis with ordered arrays of yeast deletion mutants. Science **294:**2364–2368.
64. **Tong, A. H., G. Lesage, G. D. Bader, H. Ding, H. Xu, X. Xin, J. Young, G. F. Berriz, R. L. Brost, M. Chang, Y. Chen, X. Cheng, G. Chua, H. Friesen, D. S. Goldberg, J. Haynes, C. Humphries, G. He, S. Hussein, L. Ke, N. Krogan, Z. Li, J. N. Levinson, H. Lu, P. Menard, C. Munyana, A. B. Parsons, O. Ryan, R. Tonikian, T. Roberts, A. M. Sdicu, J. Shapiro, B. Sheikh, B. Suter, S. L. Wong, L. V. Zhang, H. Zhu, C. G. Burd, S. Munro, C. Sander, J. Rine, J. Greenblatt, M. Peter, A. Bretscher, G. Bell, F. P. Roth, G. W. Brown, B. Andrews, H. Bussey, and C. Boone.** 2004. Global mapping of the yeast genetic interaction network. Science **303:**808–813.
65. **Ungar, D., T. Oka, M. Krieger, and F. M. Hughson.** 2006. Retrograde transport on the COG railway. Trends Cell Biol. **16:**113–120.
66. **Vida, T. A., and S. D. Emr.** 1995. A new vital stain for visualizing vacuolar membrane dynamics and endocytosis in yeast. J. Cell Biol. **128:**779–792.
67. **Wu, W. H., S. Alami, E. Luk, C. H. Wu, S. Sen, G. Mizuguchi, D. Wei, and C. Wu.** 2005. Swc2 is a widely conserved H2AZ-binding module essential for ATP-dependent histone exchange. Nat. Struct. Mol. Biol. **12:**1064–1071.
68. **Yang, X., R. Zaurin, M. Beato, and C. L. Peterson.** 2007. Swi3p controls SWI/SNF assembly and ATP-dependent H2A-H2B displacement. Nat. Struct. Mol. Biol. **14:**540–547.
69. **Zhang, H., D. O. Richardson, D. N. Roberts, R. Utley, H. Erdjument-Bromage, P. Tempst, J. Cote, and B. R. Cairns.** 2004. The Yaf9 component of the SWR1 and NuA4 complexes is required for proper gene expression, histone H4 acetylation, and Htz1 replacement near telomeres. Mol. Cell. Biol. **24:**9424–9436.